

# Hawking radiation for scalar fields by Einstein-Gauss-Bonnet-de Sitter black holes

Peng-Cheng Li<sup>1\*</sup> and Cheng-Yong Zhang<sup>2†</sup>

<sup>1</sup> *School of Physics and Astronomy, Sun Yat-sen University, Zhuhai 519082, China*

<sup>2</sup> *Department of Physics and Center for Field Theory and Particle Physics, Fudan University, Shanghai 200433, China*

## Abstract

We study the greybody factor and power spectra of Hawking radiation for the minimally or nonminimally coupled scalar field with exact numerical method in spherically symmetric Einstein-Gauss-Bonnet-de Sitter black hole spacetime. The effects of scalar coupling constant, angular momentum number of scalar, spacetime dimension, cosmological constant and Gauss-Bonnet coupling constant on the Hawking radiation are studied in detail. Specifically, the Gauss-Bonnet coupling constant always increases the greybody factor in the entire energy regime. Different from the case of Schwarzschild-de Sitter black hole, the effects of the scalar coupling constant on the greybody factor are not monotonic but relevant to the values of Gauss-Bonnet coupling constant. Moreover, both these two coupling constants always suppress the power spectra of Hawking radiation in the whole energy regime.

## 1 Introduction

The Einstein-Gauss-Bonnet (EGB) gravity is one of the most promising candidates for modified gravity [1]. This theory is a special case of the Lovelock gravity which is the natural generalization of general relativity in higher dimensions [2]. It has second order equations of motion and is ghost free [3]. Its action with a positive cosmological constant  $\Lambda$  in  $d$ -dimensional spacetime is

$$S_G = \frac{1}{16\pi G} \int d^d x \sqrt{-g} [R + \alpha \mathcal{L}_{GB} - 2\Lambda], \quad (1)$$

---

\*lipch7@mail.sysu.edu.cn

†zhangchengyong@fudan.edu.cn

where  $G$  is the  $d$ -dimensional Newton's constant,  $\alpha$  is the Gauss-Bonnet (GB) coupling constant of dimension  $(length)^2$ ,  $R$  is the Ricci scalar, and  $\mathcal{L}_{GB} = R_{\mu\nu\rho\sigma}R^{\mu\nu\rho\sigma} - 4R_{\mu\nu}R^{\mu\nu} + R^2$  is the so-called GB term. The GB term reduces to a topological surface term in four dimension and is only dynamical in higher dimensions. It appears as the leading order correction to the low energy effective action of the heterotic string theory [4], in which  $\alpha$  is inversely proportional to the tension of string.

The GB term is studied not only from the theoretical viewpoint, but also from phenomenological purpose. As suggested by some extra-dimension models [5, 6], the GB coupling constant may be measured by particle colliders through the Hawking radiation of tiny black holes [7–9] or in high energy cosmic-ray interactions [10, 11]. In recent years, significant number of works about the Hawking radiation in higher dimensional spacetime have been done, see the reviews [12–14]. It was shown furthermore that Hawking radiation is related to quasinormal modes and superradiance [15–18]. For more recent works, one can see [19–29].

It becomes more interesting when considering the Hawking radiation in asymptotic de Sitter (dS) spacetime. For minimally or nonminimally coupled massless scalar, the greybody factors in asymptotically flat spacetime tend to zero in the zero-frequency limit for the waves of arbitrary angular quantum number  $l$  [30–34]. However, the presence of a positive cosmological constant leads to different results. The greybody factor for the  $l = 0$  mode of a minimally coupled massless scalar by the Schwarzschild-de Sitter (SdS) black holes does not vanish in the infrared limit [35, 36]. This is due to that the zero-frequency particles are fully delocalized, and have therefore a finite probability to traverse the distance between the two horizons [36]. When the scalar is massive or equivalently the coupling is nonminimal, the infrared enhancement of transmitted flux in SdS will not present [37].

For the case of EGB gravity, the works on Hawking radiation are much less. For scalar and graviton emissions, the numerical studies of the GB black hole in an asymptotic flat spacetime were carried out in [38, 39]. Here we would like to mention that a new approximate method was adopted to obtain the analytic expressions for the greybody factors of nonminimally scalar fields by a higher dimensional Schwarzschild-dS (SdS) black hole [19]. By using the same method the study was extended to the case of EGB-dS black holes in [40]. The properties of the greybody factors and power spectra of Hawking radiation in terms of the particle and spacetime parameters were analyzed in detail. It was found that the nonminimal coupling suppresses the greybody factor and the GB coupling enhances the greybody factor, but they both suppress the energy emission rate of Hawking radiation. However, it should be pointed out that these results were obtained under the assumption that both the cosmological constant and the nonminimal coupling constant are small. Moreover, the results become problematic in the high frequency regime or in odd dimensional spacetime. In this paper, we will remedy these defects by employing exact numerical method

to study the Hawking radiation of EGB-dS black holes in the entire energy regime without any approximation imposed on the parameters. The previously obtained analytical solutions will be served as asymptotic boundary conditions here. We will compare the numerical results with the approximate analytical ones and analysis the deviations stemming from various parameters. Our study is similar to the case of SdS black holes in [20].

The outline of our paper is as follows. In Sec. 2, we present the basics of EGB-dS black hole and the equation of motion for the scalar field. In Sec. 3, we describe the numerical method solving the perturbation equation. Section 4 gives the numerical results for the greybody factor and Sec. 5 gives the numerical results for energy emission rate of Hawking radiation, on which the effects of various parameters are analyzed in detail. We summarize our results in Sec. 6.

## 2 Background

The  $d$ -dimensional spherically symmetric EGB-dS black hole solution of the theory (1) is described by [3]

$$ds^2 = -h dt^2 + \frac{dr^2}{h} + r^2 d\Omega_{d-2}^2, \quad (2)$$

$$h = 1 + \frac{r^2}{2\tilde{\alpha}} \left( 1 - \sqrt{1 + \frac{4\tilde{\alpha}m}{r^{d-1}} + \frac{8\tilde{\alpha}\Lambda}{(d-1)(d-2)}} \right).$$

Here  $d\Omega_{d-2}^2$  is the line element of the  $(d-2)$ -dimensional unit sphere  $S^{d-2}$ .  $\tilde{\alpha}$  is related to the GB coupling constant by  $\tilde{\alpha} = \alpha(d-3)(d-4)$ . The parameter  $m$  is related to the black hole mass  $M$  by  $m = \frac{16\pi GM}{(d-2)\Omega_{d-2}}$ . Depending on the parameters  $M$ ,  $\Lambda$  and  $\tilde{\alpha}$ , the black solution may have two, one or zero horizons. In this paper, we will choose parameters such that the EGB-dS black hole spacetime always has two horizons: the event horizon  $r_h$  and cosmological horizon  $r_c$ . Moreover, it was found that the EGB-dS black holes could be unstable in certain parameter regime. In our discussions, the parameters are restricted to the stable regime [41–43]. In terms of the black hole horizon radius  $r_h$ , the mass parameter  $m$  can be expressed as

$$m = r_h^{d-3} \left( 1 + \frac{\tilde{\alpha}}{r_h^2} - \frac{2\Lambda r_h^2}{(d-1)(d-2)} \right), \quad (3)$$

so that  $m$  can be eliminated from the following discussions.

We consider a massless scalar field  $\Phi$  propagating in the aforementioned EGB-dS spacetime. The scalar field is coupled minimally or nonminimally to gravity, and the corresponding action of the scalar part is

$$S_\Phi = -\frac{1}{2} \int d^d x \sqrt{-g} [\xi \Phi^2 R + \partial_\mu \Phi \partial^\mu \Phi], \quad (4)$$

where  $\xi$  is the nonminimal coupling constant, with  $\xi = 0$  corresponding to the minimally coupled case. The equation of motion of the scalar field is

$$\nabla_\mu \nabla^\mu \Phi = \xi R \Phi. \quad (5)$$

Assuming that the effect of  $\Phi$  on the background spacetime is negligible, then the above equation will be solved in a fixed background given by (2). For spherically symmetric background, we can decompose the scalar wave function as

$$\Phi = e^{-i\omega t} \phi(r) Y_{(d-2)}^l(\Omega), \quad (6)$$

where  $Y_{(d-2)}^l(\Omega)$  are spherical harmonics of the scalar wave function on  $S^{d-2}$  with angular momentum number  $l$ . The angular and the radial parts are decoupled such that the radial equation reads

$$\frac{1}{r^{d-2}} \frac{d}{dr} \left( h r^{d-2} \frac{d\phi}{dr} \right) + \left[ \frac{\omega^2}{h} - \frac{l(l+d-3)}{r^2} - \xi R \right] \phi = 0. \quad (7)$$

Here the Ricci scalar for metric (2) is

$$R = -\frac{d^2 h}{dr^2} + \frac{d-2}{r^2} \left( -2r \frac{dh}{dr} + (d-3)(1-h) \right). \quad (8)$$

Introducing a new variable  $u(r) = r^{\frac{d-2}{2}} \phi(r)$ , we get a Schrödinger-like equation

$$\frac{d^2 u}{dr_\star^2} + (\omega^2 - V(r_\star)) u = 0 \quad (9)$$

where  $r_\star$  is the tortoise coordinate defined by  $dr_\star = dr/h$ . The effective potential felt by the scalar field is

$$V(r_\star) = h \left[ \frac{l(l+d-3)}{r^2} + \xi R + \frac{d-2}{2r} h' + \frac{(d-2)(d-4)}{4r^2} h \right]. \quad (10)$$

The potential vanishes at both the event horizon and cosmological horizon of EGB-dS black hole, which allows us to analytically derive the greybody factor by using matched asymptotic expansion method [40]. In the intermediate region of these two horizons, the potential has the form of a barrier. In [40] it was revealed that due to the presence of the GB coupling constant  $\tilde{\alpha}$ , the dependence of the profile of the barrier on both spacetime and particle parameters becomes more subtle. For example, without  $\tilde{\alpha}$  the height of the barrier increase with the coupling parameter  $\xi$  of the scalar field, however, when  $\tilde{\alpha}$  has a large nonzero value,  $\xi$  suppresses the barrier. In the following we will study the effects of the various parameters on the Hawking radiation in detail.

### 3 The boundary conditions for numerical integrations

To get the information of the Hawking radiation, such as the greybody factor and power spectra of the scalar field, one should solve the radial equation (7) at first. In [40], by solving (7) near the event horizon and cosmological horizon separately and matching them in the intermediate region, they derived an approximatively analytical formula for the greybody factors when the cosmological constant and nonminimal coupling constant of the field are small. Though it is valid for all partial modes and may hold beyond the low energy regime, the deviation in the high energy regime is obvious. Besides, it works only in even dimensional spacetime. In this paper, we will solve the radial equation numerically to give the exact results and overcome the drawbacks of the approximatively analytical method.

We now briefly review the main results of the approximatively analytic approach [40]. The radial equation (7) was first solved near the event horizon. By using the coordinate transformation

$$f = \frac{h}{1 - \tilde{\Lambda}r^2}, \quad (11)$$

in which  $\tilde{\Lambda} = -\frac{1}{2\tilde{\alpha}} \left(1 - \sqrt{1 + \frac{8\tilde{\alpha}\Lambda}{(d-1)(d-2)}}\right)$  for EGB-dS black hole and imposing the ingoing boundary condition near the event horizon, the asymptotic solution has the form

$$\phi(r)|_{r \simeq r_h} = A_1 f^{\alpha_1} (1 - f)^{\beta_1} F(a_1, b_1, c_1, f), \quad (12)$$

where  $A_1$  is an arbitrary integration constant and  $F$  stands for the hypergeometric function. The expressions for parameters  $\alpha_1, \beta_1$  and hypergeometric indices  $(a_1, b_1, c_1)$  can be found in (3.9) and (3.10) in [40].

On the other hand, near the cosmological horizon by using the variable  $\tilde{h} \equiv 1 - \tilde{\Lambda}r^2$ , the radial equation (7) was solved by

$$\phi(r)|_{r \simeq r_c} = B_1 \tilde{h}^{\alpha_2} (1 - \tilde{h})^{\beta_2} F(a_2, b_2, c_2, \tilde{h}) + B_2 \tilde{h}^{-\alpha_2} (1 - \tilde{h})^{\beta_2} F(1 + a_2 - c_2, 1 + b_2 - c_2, 2 - c_2, \tilde{h}). \quad (13)$$

Here  $B_1, B_2$  are integration constant. The expressions for parameters  $\alpha_2, \beta_2$  and hypergeometric indices  $(a_2, b_2, c_2)$  are given in (3.16) and (3.18) in [40]. Note that  $\tilde{h}$  is an approximation of the metric function  $h = 1 - \tilde{\Lambda}r^2 - (r_h/r)^{d-3}(1 - \tilde{\Lambda}r^2)$  near the cosmological horizon  $r_c$ , which requires the smallness of the cosmological constant. The greybody factor for the emission of the scalar field by the black hole is determined by the amplitudes of the incoming and outgoing wave at the cosmological horizon. In term of the integration constants it is given by

$$|\gamma_{\omega l}|^2 = 1 - \left| \frac{B_2}{B_1} \right|^2. \quad (14)$$

The ratio  $B_2/B_1$  can be analytically obtained from the matching of the two asymptotic solutions (12) and (13) at intermediate regime, which occurs only if both the cosmological constant and the nonminimal coupling constant remain small. One interesting behavior of the result is that for the minimal coupling case and for the  $l = 0$  mode, the greybody factor is not vanishing even in the zero-frequency limit, similar to the SdS case. For instance, when  $l = 0$ , for small  $\tilde{\alpha}$  and in the limit  $\omega \rightarrow 0$ , one finds [40]

$$|\gamma_{\omega 0}|^2 = \frac{4(r_h r_c)^{d-2}}{(r_h^{d-2} + r_c^{d-2})^2} + \frac{4r_c^{d-2} r_h^{d-2} (r_c^{d-2} - r_h^{d-2})}{(r_c^{d-2} + r_h^{d-2})^3} \frac{\tilde{\alpha}}{r_h^2} + O(\omega, \tilde{\alpha}^2). \quad (15)$$

Since no extra approximations are made regarding the parameters, except for the smallness of the cosmological constant and the coupling constant, the above approximate method seems to be powerful, as it covers not only the most parameter regime but also the entire energy regime. However, as we will see later, its deviations from the exact solution becomes plain when moving to the high energy regime. This entails the use of the exact numerical method to solve the radial equation (7) without making any approximation for the parameters.

First of all, we determine the boundary conditions. Near the event horizon  $r \rightarrow r_h$ , we have  $f \rightarrow 0$  and the asymptotic solution 12 becomes

$$\phi(r)|_{r \rightarrow r_h} \simeq A_1 f^{\alpha_1} = A_1 e^{-i \frac{\omega r_h}{A_h} \ln f}. \quad (16)$$

Here we have used  $\alpha_1 = -i \frac{\omega r_h}{A_h}$  and  $A_h = A(r_h)$  in which

$$A(r) = -2 + \frac{d-1}{2} \left[ 1 + \left( 1 + \frac{4\tilde{\alpha}m}{(1+2\tilde{\alpha}\tilde{\Lambda})^2} \frac{1}{r^{d-1}} \right)^{-1/2} \right] (1 - \tilde{\Lambda}r^2). \quad (17)$$

The solution (16) describes an ingoing wave near the event horizon. The coefficient  $A_1$  has no specific physical significance so it can be fixed by requiring

$$\phi(r_h) = 1. \quad (18)$$

To solve (7) numerically, we still need the first derivative of  $\phi$  near the event horizon which is given by

$$\left. \frac{d\phi}{dr} \right|_{r=r_h} = A_1 e^{-i \frac{\omega r_h}{A_h} \ln f} \left( -i \frac{\omega r_h}{A_h} \right) \frac{A(r)(1-f)}{hr} \Big|_{r=r_h} \simeq -i \frac{\omega}{h(r_h)}. \quad (19)$$

Near the cosmological horizon  $r \rightarrow r_c$ , the approximation  $h \simeq 1 - \tilde{\Lambda}r^2$  will be less accurate when  $r_c$  is small or the cosmological constant is large. To avoid this, in the numerical calculations we still take  $f$  in (11) as the variable. Following a similar procedure, the asymptotic solution near

$r_c$  can be worked out as

$$\phi(r)|_{r \rightarrow r_c} = B_1 f^{\alpha_2} + B_2 f^{-\alpha_2} = B_1 e^{-i \frac{\omega r_c}{A_c} \ln f} + B_2 e^{i \frac{\omega r_c}{A_c} \ln f} \quad (20)$$

with  $\alpha_2 = -i \frac{\omega r_c}{A_c}$  in which  $A_c = A(r_c)$ . The first and second parts correspond ingoing and outgoing waves, respectively. Therefore, the greybody factor is given again by the expression (14)

Provided the boundary conditions (18) and (19), the radial equation (7) can be solved numerically from the event horizon. The numerical integrations proceed to the cosmological horizon, from which the coefficients  $B_1, B_2$  can be extracted from (20) by using

$$\begin{aligned} B_1 &= \frac{1}{2} e^{i \frac{\omega r_c}{A_c} \ln f} \left[ \phi + \frac{i A_c h r}{\omega r_c A(r) (1-f)} \frac{d\phi}{dr} \right] \Big|_{r=r_c}, \\ B_2 &= \frac{1}{2} e^{-i \frac{\omega r_c}{A_c} \ln f} \left[ \phi - \frac{i A_c h r}{\omega r_c A(r) (1-f)} \frac{d\phi}{dr} \right] \Big|_{r=r_c}. \end{aligned} \quad (21)$$

Note that as  $r \rightarrow r_h$ ,  $h(r)$  tends to 0, so that (19) tends to infinity.  $f(r)$  also tends to 0 when  $r \rightarrow r_c$  such that (21) is ill defined. We should shift the boundary from  $r = r_h$  to  $r = r_h + \epsilon$  and  $r = r_c$  to  $r = r_c - \epsilon$  to make the boundary condition manipulable. The small shift  $\epsilon$  will be chosen appropriately to assure the stability of the numerical results. In Fig. 1 we show the relative error of greybody factor and power spectra between the results when  $\epsilon = 10^{-5}$  and  $\epsilon = 10^{-8}$ . They are so small that our numerical results can be trusted.

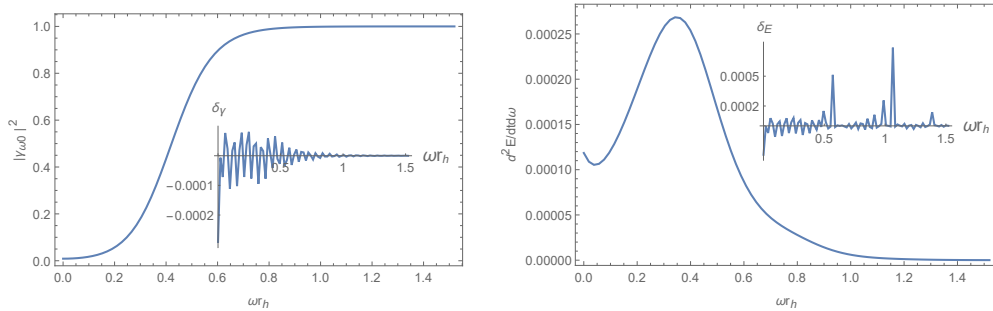


Figure 1: The greybody factor for  $l = 0$  (left) and power spectra (right) with  $d = 5$ ,  $\Lambda = 0.1$ ,  $\xi = 0$ ,  $\tilde{\alpha} = 0.6$ . The inserts show the relative errors of the greybody factor  $\delta_\gamma = \frac{|\gamma_{\omega 0}|^2_{\epsilon=10^{-5}} - |\gamma_{\omega 0}|^2_{\epsilon=10^{-8}}}{|\gamma_{\omega 0}|^2_{\epsilon=10^{-8}}}$  and the power spectra  $\delta_E = \frac{\frac{d^2 E}{dt d \omega}|_{\epsilon=10^{-5}} - \frac{d^2 E}{dt d \omega}|_{\epsilon=10^{-8}}}{\frac{d^2 E}{dt d \omega}|_{\epsilon=10^{-8}}}$ , respectively.

## 4 Greybody factor

### 4.1 Comparison of numerical and analytical results

With the numerical result at our disposal, we can compare it with the analytical expression for the greybody factor derived in [40]. In Fig. 2, we plot the numerical and analytical results for the greybody factors for different values of the cosmological constant  $\Lambda$  and the nonminimal coupling constant  $\xi$ . They are in well agreement in the low energy regime. However, the deviations of the approximatively analytical results from the exact numerical results become evident as  $\xi$  or  $\Lambda$  increases. This is expected since it was assumed small  $\xi$  and  $\Lambda$  to get the analytical expression of greybody factors in [40].

On the other hand, the greybody factor should tend to 1 when the energy is large enough no matter what value  $\xi$  or  $\Lambda$  takes, as shown by the numerical result in Fig. 2. This is due to the fact that the particle with high energy can overcome the effective potential barrier easily and escape to far region. However, the analytical result tends to 0 in the high energy regime and thus become unreliable at all. We will show only the effects of various parameters on the numerical result hereafter, since it is valid over the entire energy regime and for arbitrary values of the particle and spacetime parameters.

Moreover, the greybody factors for odd dimensional spacetime cannot be obtained from the approximatively analytical method in [40]. The numerical method here can remedy this flaw and the effects of dimension will be analyzed in subsection 4.4. Hereafter, we focus mainly on the odd dimensional spacetime to emphasize the new results.

Without the GB term in the theory, the dependence of the greybody factors on the various parameters has been studied numerically in [20]. The results can be summarized as follows. The greybody factor is suppressed by the angular momentum number  $l$ , both for minimally or non-minimally coupled scalar. The similar case occurs for the spacetime dimensions  $d$ . Moreover, the nonminimal coupling constant  $\xi$  decreases the greybody factor when other parameters are fixed. The effect of the cosmological constant on the greybody factor depends on the value of  $\xi$ . The cosmological constant enhances the greybody factor for small  $\xi$ , but for large  $\xi$  it leads to a suppression in the greybody factor especially in the low-energy regime. As we will see in the following, the presence of the GB term in the theory makes the analysis more subtle than the case of general relativity.

### 4.2 Effects of $\tilde{\alpha}$ on the greybody factor for different partial modes $l$

In this subsection, we study the effect of  $\tilde{\alpha}$  on the greybody factor for different partial modes  $l$ . We take  $d = 5$  for example. The behaviors in other dimensions are qualitatively similar. From the left panel of Fig. 3, we see that the greybody factor is suppressed significantly as  $l$  increases



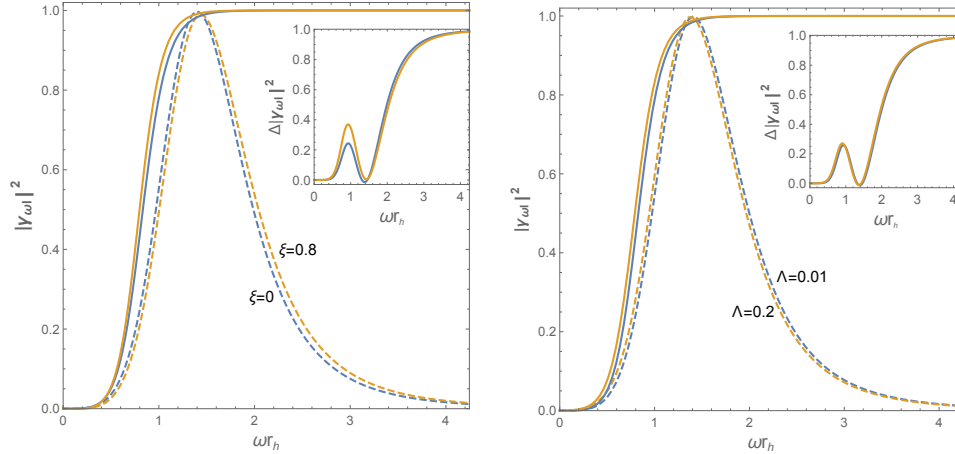


Figure 2: Analytical (dashed lines) and numerical (solid lines) results for the greybody factors when  $d = 6, l = 0, \tilde{\alpha} = 0.5$ . Left panel for  $\Lambda = 0.01$ . Blue lines for  $\xi = 0$ , yellow lines for  $\xi = 0.8$ . Right panel for  $\xi = 0.1$ . Blue lines for  $\Lambda = 0.01$ , yellow lines for  $\Lambda = 0.2$ . The inserts show the difference of greybody factors  $\Delta|\gamma_{\omega l}|^2 = |\gamma_{\omega l}|^2_{\text{numerical}} - |\gamma_{\omega l}|^2_{\text{analytical}}$  between numerical result and analytical result with the same parameters.

with other parameters fixed. As a consequence, the mode  $l = 0$  dominates the radiation. On the other hand,  $\tilde{\alpha}$  increases the greybody factors for all modes  $l$  in the whole energy regime. We find that this qualitative behavior is independent of the spacetime dimension  $d$ , scalar coupling  $\xi$  and cosmological constant  $\Lambda$ . In the right panel, we plot the corresponding effective potential to understand this behavior intuitively. For larger  $l$ , when other parameters are fixed, the wave must transverse a higher effective potential barrier, thus its transmission is suppressed with  $l$ . At the meantime,  $\tilde{\alpha}$  always decreases the effective potential barrier so that it becomes easier for the scalar to transverse the barrier and the greybody factor increases with  $\tilde{\alpha}$ .

### 4.3 Competition between $\xi$ and $\tilde{\alpha}$

As we mentioned before the nonminimally coupling  $\xi$  suppresses the greybody factor while the GB parameter  $\tilde{\alpha}$  enhances it, thus there must be a competition between them. From Fig. 4, we see that when  $\tilde{\alpha}$  is small (left panel),  $\xi$  decreases the greybody factor for all modes  $l$  in the entire energy regime. The situation becomes involved when  $\tilde{\alpha}$  is large (right panel). In the low energy regime,  $\xi$  still decreases the greybody factor. However, it enhances the greybody factor in the high energy regime. This behavior exists for all  $l$  in  $d \geq 5$  EGB dS black hole spacetime. This phenomenon has an intuitive explanation from the effective potential. From Fig. 5, we find that when  $\tilde{\alpha}$  is small,  $\xi$  increases the effective potential and hence suppresses the greybody factor. When  $\tilde{\alpha}$  is large,  $\xi$  decreases the effective potential and enhances the greybody factor. This is different from the Schwarzschild-de Sitter black hole where  $\xi$  always suppresses the greybody factor [20].

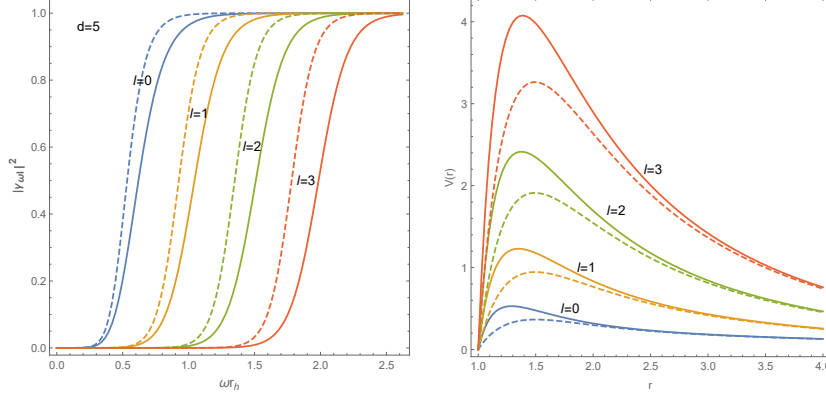


Figure 3: Effect of  $\tilde{\alpha}$  on the greybody factor for different mode  $l$  and the corresponding effective potential. Solid lines for  $\tilde{\alpha} = 0$ , dashed lines for  $\tilde{\alpha} = 0.3$ . We fix  $d = 5$ ,  $\Lambda = 0.1$ ,  $\xi = 0.6$  here.

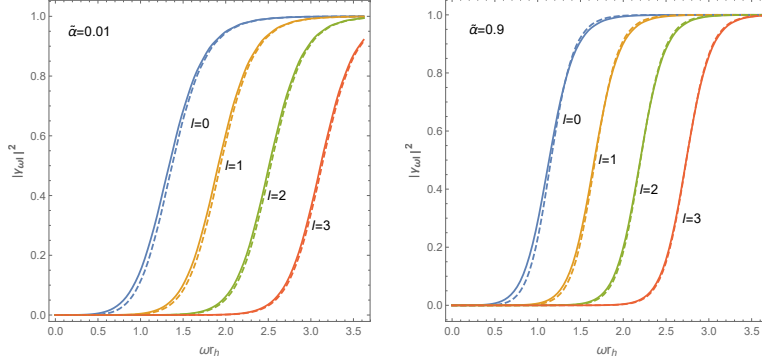


Figure 4: Effect of  $\xi$  on the greybody factor for different  $l$ . Solid lines for  $\xi = 0$ , dashed lines for  $\xi = 0.6$ . We fix  $d = 7$ ,  $\Lambda = 0.1$  here.

#### 4.4 Effects of $d$ on the greybody factor

Now let us study the dependence of the greybody factor on the spacetime dimensions  $d$  in the presence of  $\tilde{\alpha}$ . In Fig. 6, we depict the effects of the dimensions  $d$  on the greybody factor for dominant mode  $l = 0$ . Note that we can obtain the greybody factors for spacetime with odd dimension  $d$  here which is absent in the approximatively analytical method in [40] due to the poles of the Gamma function. It is obvious that the greybody factor is significantly suppressed in higher dimensions. Furthermore, we find similar behaviors as in subsection 4.3: when  $\tilde{\alpha}$  is small, the scalar coupling constant  $\xi$  always decreases the greybody factor. When  $\tilde{\alpha}$  is large,  $\xi$  decreases the greybody factor only in the low energy regime but increases the greybody factor in the high energy region. The behaviors of the effective potential are also similar with those in Fig. 5.

Note that when  $\omega \rightarrow 0$ , the greybody factor is nonzero for dominant mode  $l = 0$  for minimally coupled scalar. For  $d = 5, 6, 7, 8, 9$  as examples, when  $\Lambda = 0.1$ , the greybody factors have values of order  $10^{-3}, 10^{-4}, 10^{-5}, 10^{-7}, 10^{-8}$ , respectively.

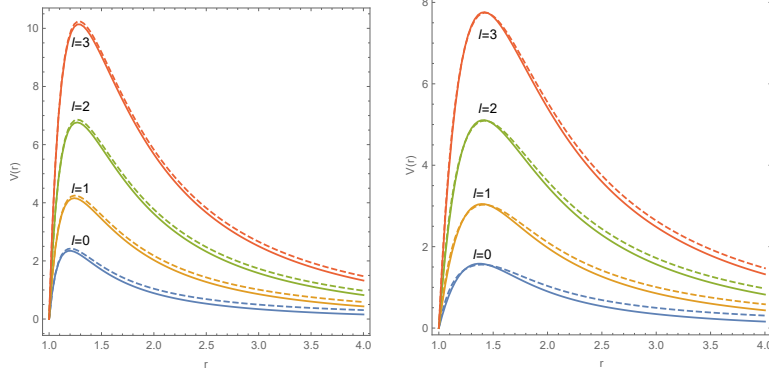


Figure 5: Effective potential of the scalar with the corresponding parameters in Fig . 4.

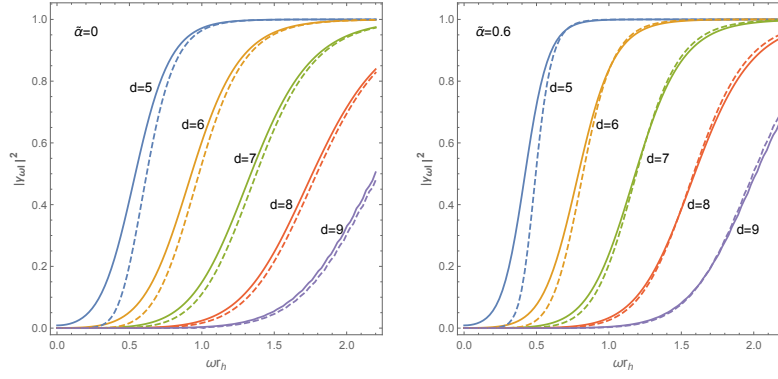


Figure 6: Effect of  $d$  on the greybody factor. Solid lines for  $\xi = 0$ , dashed lines for  $\xi = 0.6$ . We fix  $l = 0, \Lambda = 0.1$  here. The small wiggles for  $d = 9$  is caused by the numerical error.

#### 4.5 Competition between $\Lambda$ and $\xi$ in the presence of $\tilde{\alpha}$

As can be seen from Fig. 7,  $\Lambda$  increases the greybody factor when  $\xi$  is small in the whole energy regime (left panel). When  $\xi$  is large (right panel),  $\Lambda$  decreases the greybody factor, mainly in the low and intermediate energy regime. This behavior has been found in [40] by using approximate analytical method which is reliable only in low energy regime there. This phenomenon can be understood from the double roles  $\Lambda$  plays. The positive cosmological constant behaves like an homogenously distributed energy in the spacetime. It increases the effective energy of the particles, making it easier to pass through the effective potential barrier. Hence it can enhance the greybody factor. On the other hand, it couples to  $\xi$  in the equation of motion (5) and behaves as an effective mass for the particles, making it harder to transverse the effective potential. Hence it can also suppress the greybody factor. For small  $\xi$ , the suppression due to the effective mass is also small, as a consequence the enhancement effect of cosmological constant dominates the process. For large  $\xi$ , the effective mass increases substantially with  $\Lambda$ , thus the greybody factor is suppressed. This phenomenon is also discovered in other dimensions. We find that this competition behavior of  $\Lambda$

and  $\xi$  is independent of the GB coupling  $\tilde{\alpha}$ .

Similarly, the effect of  $\tilde{\alpha}$  on the greybody factor as analyzed in 4.2 could be explained from a more physical way. First, from the field equations of the theory (1)

$$R_{\mu\nu} - \frac{1}{2}Rg_{\mu\nu} + \Lambda g_{\mu\nu} + \alpha H_{\mu\nu} = 0, \quad (22)$$

where

$$H_{\mu\nu} = -\frac{1}{2}g_{\mu\nu}\mathcal{L}_{GB} + 2(RR_{\mu\nu} - 2R_{\mu\gamma}R^\gamma_\nu + 2R^{\gamma\delta}R_{\gamma\mu\nu\delta} + R_{\mu\gamma\delta\lambda}R_\nu^{\gamma\delta\lambda}), \quad (23)$$

formally, one may treat  $-\alpha H_{\mu\nu}$  as an effective stress tensor. Then from this point of view, the quantity  $\alpha H_{tt}$  can be regarded as a local energy density. It is straightforward to check that this quantity is always positive for a positive  $\alpha$ , which as a result could increase the effective energy of the particles and enhance its ability of tunneling through the effective potential barrier.

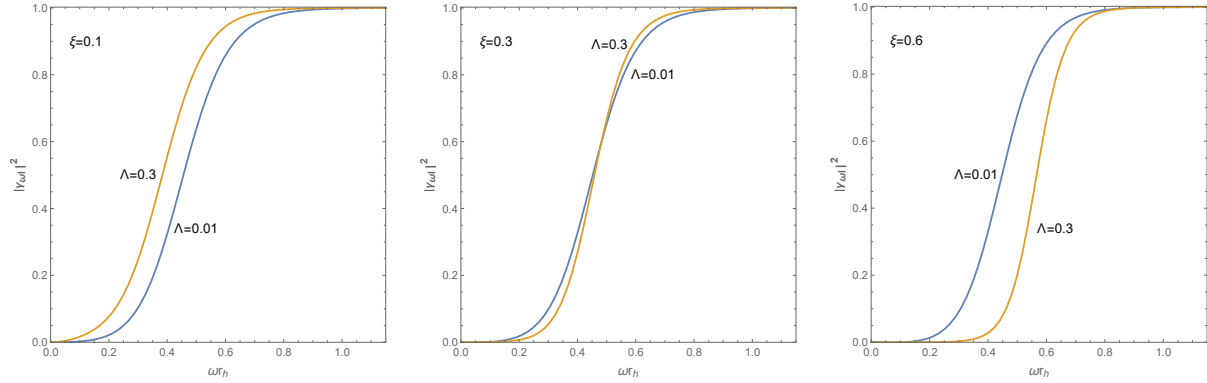


Figure 7: Competition between  $\Lambda$  and  $\xi$  in the presence of  $\tilde{\alpha}$ . The greybody factors for  $d = 5, l = 0, \tilde{\alpha} = 0.6$  with respect to  $\Lambda = 0.01, 0.3$  and  $\xi = 0.1, 0.3, 0.6$ .

## 5 Energy emission rate of Hawking radiation

The greybody factor reflects only the transmissivity of a particular mode. A more comprehensive quantity that characterizes the Hawking radiation is the energy emission rate, i.e., the power spectra for the emission. The differential energy emission rate is given by [6, 33, 36]

$$\frac{d^2 E}{dt d\omega} = \frac{1}{2\pi} \sum_l \frac{N_l |\gamma_{\omega l}|^2 \omega}{e^{\omega/T} - 1}, \quad (24)$$

where  $N_l = \frac{(2l+d-3)(l+d-4)!}{l!(d-3)!}$  is the multiplicity of states that have the same  $l$ .  $T$  is the temperature of the system. For black hole spacetime, it is usually defined as  $T_0 = \frac{\kappa_h}{2\pi}$ , where  $\kappa_h$  is the surface gravity of the event horizon. However, this definition is valid only in asymptotically flat spacetime [44]. For asymptotic dS spacetime, various definitions of temperature were proposed. Here we will

consider six different temperatures and study their influences on the power spectra of Hawking radiation. The normalized temperature that proposed in [44] is

$$T_{BH} = \frac{1}{\sqrt{h(r_0)}} \frac{\kappa_h}{2\pi}, \quad (25)$$

where  $r_0$  is the position where  $h(r)$  is extreme. The black hole attraction balances the cosmological repulsion near this point such that the spacetime is almost flat there. For dS black hole, there is cosmological horizon temperature defined as  $T_c = -\frac{\kappa_c}{2\pi}$ , where  $\kappa_c$  is the surface gravity of the cosmological horizon. In general,  $T_0$  and  $T_c$  are different, thus the spacetime is not in equilibrium. Some effective temperatures inspired from the black hole thermodynamics were proposed to resolve this problem (See [20–22, 44] for more information):

$$T_{effEIW} = \frac{r_h^4 T_c + r_c^4 T_0}{(r_h + r_c)(r_c^3 - r_h^3)}, \quad T_{effBH} = \left( \frac{1}{T_c} - \frac{1}{T_{BH}} \right)^{-1}, \quad (26)$$

$$T_{eff-} = \left( \frac{1}{T_c} - \frac{1}{T_0} \right)^{-1}, \quad T_{eff+} = \left( \frac{1}{T_c} + \frac{1}{T_0} \right)^{-1}. \quad (27)$$

We show their dependence on  $\Lambda$  in Fig. 8 when  $d = 5$ . When  $\tilde{\alpha}$  is small,  $T_{BH}$  dominates in the whole  $\Lambda$  region. If  $\tilde{\alpha}$  is large,  $T_{eff-}$  becomes dominant for large  $\Lambda$ . However,  $T_{eff-}$  jumps to be negative when  $\tilde{\alpha}$  exceeds a critical value where  $T_0$  becomes smaller than  $T_c$  in the parameter region shown in the right panel of Fig. 8. The greater  $\Lambda$  is, the smaller critical  $\tilde{\alpha}$ . When  $d > 5$ , it can be shown that there is always  $T_0 > T_c$  such that  $T_{eff-}$  is always positive. Moreover, we find that when  $\Lambda \rightarrow 0$ ,  $T_{eff-}, T_{effBH}, T_{eff+}$  all tend to 0. This will lead to vanishing radiation in asymptotically flat spacetime and is unreasonable. Thus we will take  $T_{BH}, T_{effEIW}$  as the temperature in (24).

Figure 9 shows the influence of  $\tilde{\alpha}$  on temperature when  $d = 6$ . We find that  $T_{BH}, T_{effEIW}$  all decrease with  $\tilde{\alpha}$  no matter whether  $\Lambda$  is small or large. This behavior is also observed in other dimensions. This enables us to take  $T_{BH}$  as example to study the power spectra of Hawking radiation. The qualitative behavior of power spectra with respect to  $\tilde{\alpha}$  will not change if  $T_0$  or  $T_{effEIW}$  is adopted. In the following, we will only show the results of  $d = 5$  in most part of this section for convenience. Qualitatively similar behaviors are observed in higher dimensions.

Substituting these temperatures into (24), we get the power spectra shown in Fig. 10 and Fig. 11 for examples. For minimally coupled scalar, the power spectra in the low energy limit is finite, while the power spectra for nonminimally coupled scalar in the low energy limit vanishes. This is due to the nonvanishing greybody factors for the dominant mode  $l = 0$  of minimally coupled scalar, as shown in (15).

Moreover, We can see that only  $T_{BH}$  leads to significant radiation both for small  $\Lambda$  and large  $\Lambda$ . We therefore take this temperature to study the effects of other parameters on the Hawking radiation hereafter.

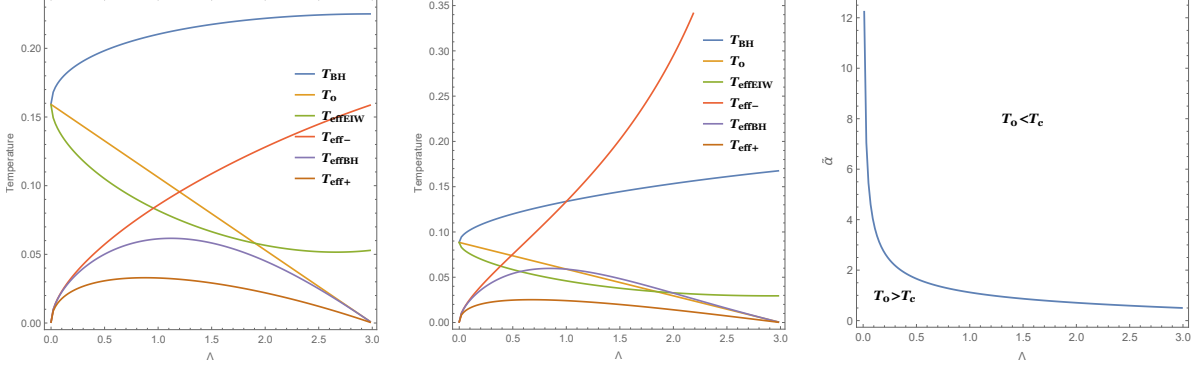


Figure 8: Different temperatures with respect to  $\Lambda$  when  $d = 5$ . The extremal cosmological constant is  $\Lambda = 3$  where  $r_c = r_h$ . Left panel for  $\tilde{\alpha} = 0$ , middle panel for  $\tilde{\alpha} = 0.4$ , right panel for the critical curve where  $T_0 = T_c$ . In higher dimensions, there is always  $T_0 > T_c$ .

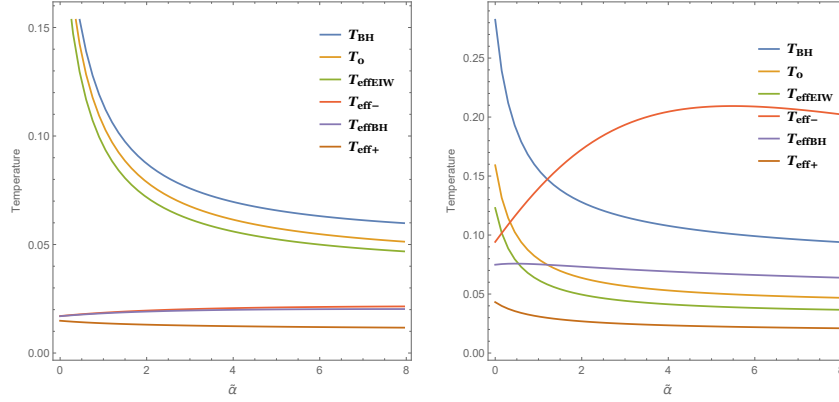


Figure 9: Different temperatures with respect to  $\tilde{\alpha}$  when  $d = 6$ . The extremal cosmological constant is  $\Lambda = 6 + 2\tilde{\alpha}$ . Left panel for  $\Lambda = 0.1$ , right panel for  $\Lambda = 1$ .

The contribution to the energy emission rate comes mainly from lower modes  $l$  [20, 40], as shown in Fig. 12 for example. Without loss of validness, we could omit the contributions from modes  $l > 6$  in (24) hereafter.

### 5.1 Effects of $\tilde{\alpha}$ and $\xi$ on the power spectra of Hawking radiation

We study the effects of  $\tilde{\alpha}$  and  $\xi$  on the power spectra of Hawking radiation in this subsection. From the left panel of Fig. 13, we see that  $\tilde{\alpha}$  suppresses the power spectra in the whole energy regime. This may be surprised since we have found that  $\tilde{\alpha}$  decreases the greybody factor in the entire energy regime in subsection 4.2. In fact, the power spectra depends also on the normalized temperature  $T_{BH}$ . The significant suppression of the power spectra with  $\tilde{\alpha}$  is due to the decrease of  $T_{BH}$  as shown in Fig. 9.

On the other hand, in subsections 4.3 and 4.4, we found that  $\xi$  could increase the greybody factor in the high energy regime when  $\tilde{\alpha}$  is large enough. However, we find that  $\xi$  always suppresses

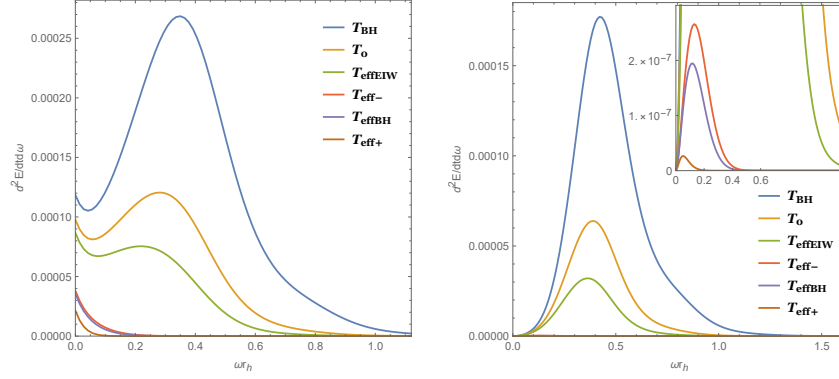


Figure 10: Power spectra for different temperatures. Left panel for  $\xi = 0$ , right panel for  $\xi = 0.3$ . We fix  $d = 5$ ,  $\Lambda = 0.1$ ,  $\tilde{\alpha} = 0.6$  here.

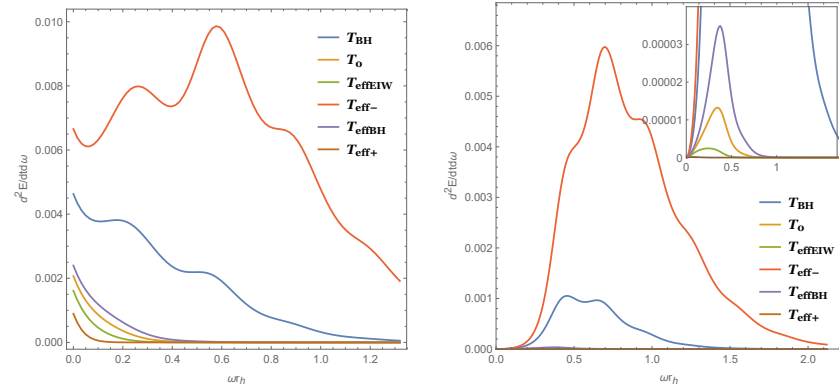


Figure 11: Power spectra for different temperatures. Left panel for  $\xi = 0$ , right panel for  $\xi = 0.3$ . We fix  $d = 5$ ,  $\Lambda = 0.9$ ,  $\tilde{\alpha} = 0.6$  here.

the power spectra in the whole energy regime, as shown in the right panel of Fig. 13. We find that this qualitative behavior is independent of  $\tilde{\alpha}$ . Moreover, when other parameters are fixed, the peak of the power spectra moves to lower frequency when  $\tilde{\alpha}$  increases, or to the higher frequency when  $\xi$  increases. These behaviors are in accordance with those found in [40] by using approximative analytical method.

Note that when  $\xi = 0$ , the power spectra is nonzero when  $\omega \rightarrow 0$  due to the nonvanishing of greybody factor for dominant mode  $l = 0$ . It decreases monotonically with  $\tilde{\alpha}$  as shown in Fig. 14.

## 5.2 Effects of $d$ on the power spectra of Hawking radiation

The effect of spacetime dimension  $d$  on the power spectra of Hawking radiation is shown in Fig. 15. Although the greybody factor is suppressed by  $d$  as shown in subsection 4.4, the significant increase of  $T_{BH}$  leads to the overall enhancement of the power spectra. This phenomenon has been found in [20, 33, 36]. We also see that the peak of the power spectra moves to higher frequency in higher dimensions.

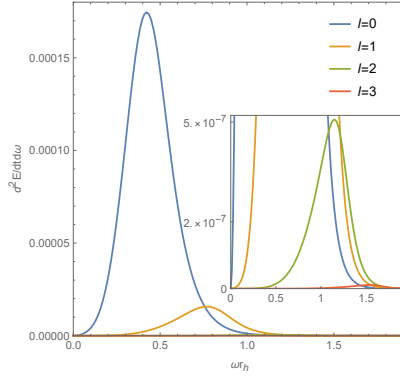


Figure 12: The contributions from different  $l$ . We fix  $d = 5, \xi = 0.3, \tilde{\alpha} = 0.3, \Lambda = 0.1$  here. Note that the contribution from  $l = 3$  is of order  $10^{-8}$ .

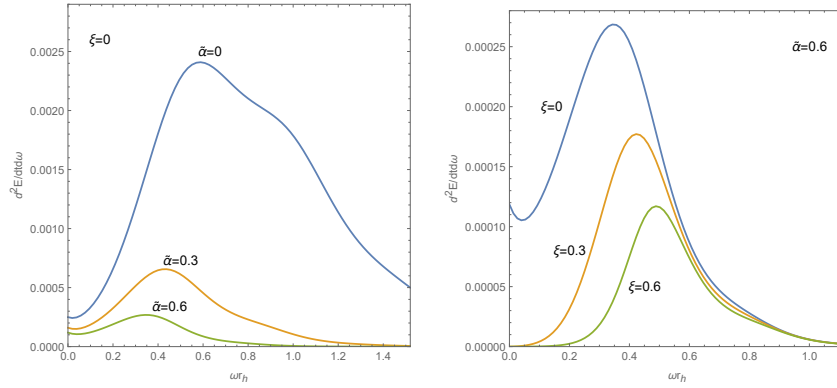


Figure 13: Effect of  $\tilde{\alpha}$  and  $\xi$  on the power spectra of Hawking radiation. We fix  $d = 5, \Lambda = 0.1$  here.

### 5.3 Competition between $\xi$ and $\Lambda$

From Fig. 16, we find that, when  $\xi$  is small, the power spectra is enhanced by  $\Lambda$  in the whole energy regime. For intermediate value of  $\xi$ , the enhancement occurs only in the higher energy regime. When  $\xi$  is large, besides the enhancement in the high energy regime, the power spectra is actually suppressed in the low energy regime as  $\Lambda$  increases. This phenomenon has been found for SdS black hole [20]. Note that the GB coupling  $\tilde{\alpha}$  does not change this behavior qualitatively. The low energy behavior has also been discussed in [40].

## 6 Summary

We performed a comprehensive study of the greybody factors and power spectra of Hawking radiation for the nonminimally coupled scalar field numerically in spherically symmetric EGB-dS black hole spacetime. A recent work [40] had addressed the same problem in an approximate analytical way, however, the validity of this method relied on the assumption that both the cosmo-



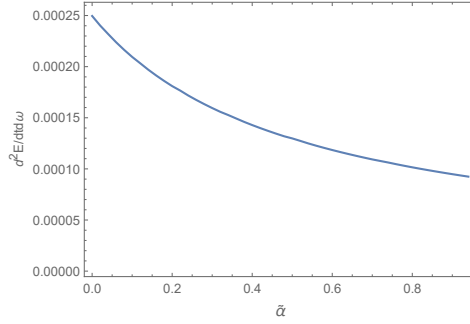


Figure 14: Effect of  $\tilde{\alpha}$  on the power spectra in the low energy limit. We fix  $d = 5, \Lambda = 0.1, \xi = 0$  here. The behavior in higher dimensional spacetime is qualitative similar.

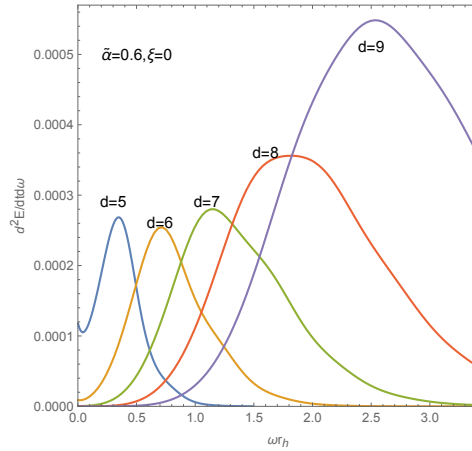


Figure 15: Effects of  $d$  on the power spectra of Hawking radiation. We fix  $\Lambda = 0.1$  here.

logical constant and the nonminimal coupling were small. In this work, by numerically solving the scalar field equation and without making any approximation for the parameters we obtained the exact results for the greybody factors and Hawking radiation spectra in the entire energy regime. The approximate analytical solutions [40] can be served as asymptotic boundary conditions for our numerical integrations.

We first compared our results with the ones obtained by approximate analytical method in [40]. In the low energy regime, these two set of results agree well for small cosmological constant  $\Lambda$  and nonminimal coupling constant  $\xi$ . The deviations become large when  $\Lambda$ ,  $\xi$  or the energy of the emitted particle increase beyond the allowed regime.

The numerical results show that the greybody factor is suppressed significantly by both the spacetime dimensions  $d$  and the angular momentum number  $l$  of the scalar. The GB coupling  $\tilde{\alpha}$  always increases the greybody factor when other parameters are fixed. The effects of scalar coupling  $\xi$  on the greybody factor are relevant to the GB coupling  $\tilde{\alpha}$ . However, when  $\tilde{\alpha}$  is small,  $\xi$  decreases the greybody factor in the whole energy regime. When  $\tilde{\alpha}$  is large,  $\xi$  decreases the greybody factor

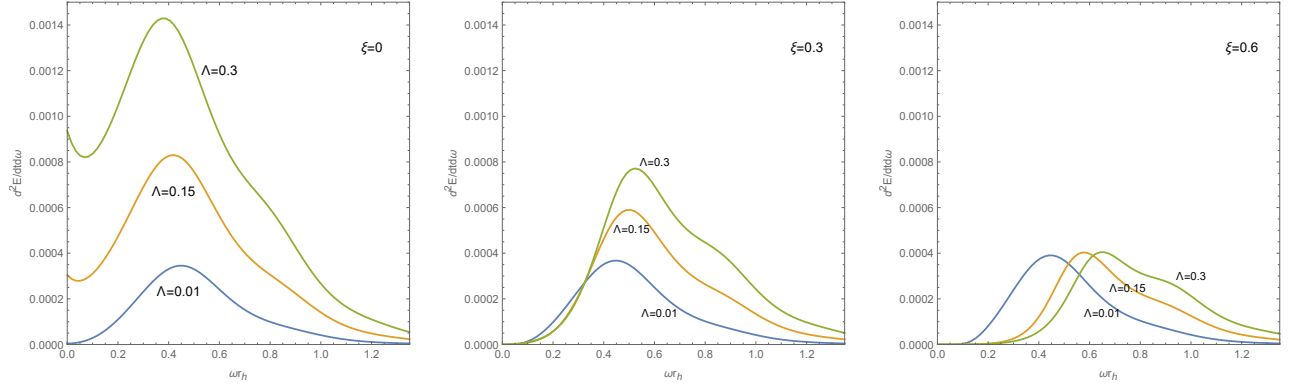


Figure 16: Effects of  $\Lambda$  on the power spectra of Hawking radiation. We fix  $d = 5, \tilde{\alpha} = 0.3$  here.

only in the low energy regime but increases the greybody factor in the high energy regime instead. This is different from the case of Schwarzschild-de Sitter black hole where  $\xi$  always decreases the greybody factor [20]. The effects of cosmological constant on the greybody factor are relevant to scalar coupling constant: depending on the value of the nonminimal coupling constant, the positive  $\Lambda$  can either help or hinder the particle to overcome the potential barrier. This phenomenon is due to the competition between the two roles  $\Lambda$  plays: it subsidize energy to the particle and also the effective mass of the particle.

We also analyzed the effects of  $d, \xi, \tilde{\alpha}, \Lambda$  on the energy emission rate of Hawking radiation in detail. The energy emission rate depends on both the greybody factor and the black hole temperature. For dS black holes, the definition of temperature is subtle. We compared various temperature definitions and find that the normalized temperature is the most natural one for studying Hawking radiation. The normalized temperature decreases with  $\alpha$ . As a result, due to the dominant role of temperature on Hawking radiation, we found that both  $\tilde{\alpha}$  and  $\xi$  suppress the power spectra, unlike their subtle effects on the greybody factor. Moreover, the power spectra is overall enhanced significantly as  $d$  increases and the peak moves to higher energy regime. The effect of  $\Lambda$  on the power spectra is relevant to the scalar coupling constant too. When  $\xi$  is small, it increases the power spectra in the whole energy region. When  $\xi$  is large, it increases the power spectra only in higher energy regime and instead decreases the power spectra in the lower energy regime.

## 7 Acknowledgments

P.-C. Li is supported by NSFC Grant No. 11847241. C.-Y. Zhang is supported by National Postdoctoral Program for Innovative Talents BX201600005 and Project funded by China Postdoctoral Science Foundation.

## References

- [1] T. Clifton, P. G. Ferreira, A. Padilla, C. Skordis, “Modified Gravity and Cosmology,” *Phys.Rept.* 513 (2012) 1-189. arXiv:1106.2476.
- [2] D. Lovelock, “The Einstein tensor and its generalizations,” *J.Math.Phys.* 12 (1971) 498-501.
- [3] B. Zwiebach. “Curvature Squared Terms and String Theories,” *Phys. Lett.*, B156:315, 1985.
- [4] D. G. Boulware and S. Deser, “String-Generated Gravity Models,” *Phys. Rev. Lett.* 55, 2656 (1985).
- [5] A. Barrau, J. Grain, and S. O. Alexeyev, “Gauss-Bonnet black holes at the LHC: Beyond the dimensionality of space,” *Phys. Lett. B* **584**, 114 (2004), arXiv:hep-ph/0311238.
- [6] P. Kanti, “Black Holes in Theories with Large Extra Dimensions: a Review,” *Int. J. Mod. Phys. A* 19 (2004) 4899-4951, arXiv:hep-ph/0402168.
- [7] S. Dimopoulos and G. L. Landsberg, “Black Holes at the LHC,” *Phys. Rev. Lett.* 87, 161602 (2001), arXiv:hep-ph/0106295.
- [8] D.-C. Dai, G. Starkman, D. Stojkovic, C. Issever, E. Rizvi, and J. Tseng, “BlackMax: A black-hole event generator with rotation, recoil, split branes, and brane tension,” *Phys. Rev. D* 77, 076007 (2008), arXiv:0711.3012.
- [9] P. Kanti, “Black holes at the LHC,” *Lect. Notes Phys.* 769, 387 (2009), arXiv:0802.2218.
- [10] J. L. Feng and A. D. Shapere, “Black Hole Production by Cosmic Rays,” *Phys. Rev. Lett.* 88, 021303 (2001), arXiv:hep-ph/0109106.
- [11] R. Emparan, M. Masip, and R. Rattazzi, “Cosmic rays as probes of large extra dimensions and TeV gravity,” *Phys. Rev. D* 65, 064023 (2002), arXiv:hep-ph/0109287.
- [12] P. Kanti, “Black Holes in Theories with Large Extra Dimensions: a Review,” *Int. J. Mod. Phys. A* 19 (2004) 4899-4951, arXiv:hep-ph/0402168.
- [13] T. Harmark, J. Natario, R. Schiappa, “Greybody Factors for d-Dimensional Black Holes,” *Adv. Theor. Math. Phys.* **14** (2010) no.3, 727-794, arXiv:0708.0017.
- [14] P. Kanti, E. Winstanley, “Hawking Radiation from Higher-Dimensional Black Holes,” *Fundam. Theor. Phys.* **178** (2015) 229-265, arXiv:1402.3952.
- [15] James W. York, Jr., “Dynamical origin of black-hole radiance,” *Phys. Rev. D* 28, 2929 (1983).

- [16] O. J. C. Dias, R. Emparan, and A. Maccarrone, “Microscopic theory of black hole super-radiance”, *Phys.Rev. D* **77** (2008) 064018, arXiv:0712.0791.
- [17] E. Berti, V. Cardoso and A. O. Starinets, “Quasinormal modes of black holes and black branes,” *Class. Quant. Grav.* **26**, 163001 (2009), arXiv:0905.2975.
- [18] R. Brito, V. Cardoso and P. Pani, “Superradiance: Energy Extraction, Black-Hole Bombs and Implications for Astrophysics and Particle Physics”, *Lect. Notes Phys.* **906**, pp.1 (2015), arXiv:1501.06570.
- [19] P. Kanti, T. Pappas, and N. Pappas, “Greybody factors for scalar fields emitted by a higher-dimensional Schwarzschild-de-Sitter black-hole,” *Phys. Rev. D* **90**, 124077 (2014), arXiv:1409.8664.
- [20] T. Pappas, P. Kanti and N. Pappas, “Hawking Radiation Spectra for Scalar Fields by a Higher-Dimensional Schwarzschild-de-Sitter Black Hole,” *Phys. Rev. D* **94** (2016) no.2, 024035, arXiv:1604.08617.
- [21] P. Kanti and T. Pappas, “Effective temperatures and radiation spectra for a higher-dimensional Schwarzschild-de Sitter black hole,” *Phys. Rev. D* **96** (2017) no.2, 024038, arXiv:1705.09108.
- [22] T. Pappas, P. Kanti, “Schwarzschild-de Sitter spacetime: The role of temperature in the emission of Hawking radiation,” *Phys.Lett. B* **775** (2017) 140-146, arXiv:1707.04900.
- [23] R. Jorge, E. S. de Oliveira, and J. V. Rocha, “Greybody factors for rotating black holes in higher dimensions,” *Classical Quantum Gravity* **32**, 065008 (2015).
- [24] R. Dong and D. Stojkovic, “Greybody factors for a black hole in massive gravity,” *Phys. Rev. D* **92**, 084045 (2015).
- [25] J. Ahmed and K. Saifullah, “Greybody factor of scalar field from Reissner-Nordstrom-de Sitter black hole,” *Eur. Phys. J. C* **78** (2018) no.4, 316, arXiv: 1610.06104.
- [26] G. Panotopoulos and A. Rincon, “Greybody factors for a nonminimally coupled scalar field in BTZ black hole background,” *Phys. Lett. B* **772**, 523 (2017), arXiv:1611.06233.
- [27] X.-M. Kuang, J. Saavedra, A. Övgün, “The Effect of the Gauss-Bonnet term to Hawking Radiation from arbitrary dimensional Black Brane,” *Eur. Phys. J. C* **77** (2017) no.9, 613, arXiv:1707.00169.
- [28] C. Y. Zhang, S. J. Zhang and B. Wang, “Charged scalar perturbations around Garfinkle-Horowitz-Strominger black holes,” *Nucl. Phys. B* **899**, 37 (2015), arXiv:1501.03260.

- [29] C. Y. Zhang, S. J. Zhang and B. Wang, “Superradiant instability of Kerr-de Sitter black holes in scalar-tensor theory,” JHEP **1408**, 011 (2014), arXiv:1405.3811.
- [30] D. N. Page, “Particle emission rates from a black hole: Massless particles from an uncharged, nonrotating hole,” Phys. Rev. D **13**, 198 (1976).
- [31] S. R. Das, G. Gibbons, and S. D. Mathur, “Universality of Low Energy Absorption Cross-sections for Black Holes,” Phys. Rev. Lett. **78**, 417 (1997), arXiv:hep-th/9609052.
- [32] A. Higuchi, “Low frequency scalar absorption cross-sections for stationary black holes,” Classical Quantum Gravity **18**, L139 (2001); 19, 599 (2002), arXiv:hep-th/0108144.
- [33] C. M. Harris and P. Kanti, “Hawking radiation from a  $(4+n)$ -dimensional black hole: Exact results for the Schwarzschild phase,” JHEP **0310** (2003) 014, arXiv:hep-ph/0309054.
- [34] S. Chen and J. Jing, “Greybody factor for a scalar field coupling to Einstein’s tensor,” Phys. Lett. B **691**, 254 (2010), arXiv:1005.5601.
- [35] P. R. Brady, C. M. Chambers, W. Krivan, and P. Laguna, “Telling tails in the presence of a cosmological constant,” Phys. Rev. D **55**, 7538 (1997), arXiv:gr-qc/9611056.
- [36] P. Kanti, J. Grain, A. Barrau, “Bulk and Brane Decay of a  $(4+n)$ -Dimensional Schwarzschild-De-Sitter Black Hole: Scalar Radiation,” Phys. Rev. D **71** (2005) 104002, arXiv:hep-th/0501148.
- [37] L. C. B. Crispino, A. Higuchi, E. S. Oliveira, and J. V. Rocha, “Greybody factors for nonminimally coupled scalar fields in Schwarzschild-de Sitter spacetime,” Phys. Rev. D **87**, 104034 (2013), arXiv:1304.0467.
- [38] J. Grain, A. Barrau, and P. Kanti, “Exact results for evaporating black holes in curvature-squared lovelock gravity: Gauss-Bonnet greybody factors,” Phys. Rev. D **72**, 104016 (2005), arXiv:hep-th/0509128.
- [39] R. A. Konoplya and A. Zhidenko, “Long life of Gauss-Bonnet corrected black holes,” Phys. Rev. D **82**, 084003 (2010), arXiv:1004.3772.
- [40] C.-Y. Zhang, P.-C. Li and B. Chen, “Greybody factors for Spherically Symmetric Einstein-Gauss-Bonnet-de Sitter black hole,” Phys. Rev. D **97** (2018) no.4, 044013, arXiv:1712.00620.
- [41] R. A. Konoplya and A. Zhidenko, “(In)stability of D-dimensional black holes in Gauss-Bonnet theory,” Phys. Rev. D **77** (2008) 104004, arXiv:0802.0267.

- [42] M. A. Cuyubamba, R. A. Konoplya and A. Zhidenko, “Quasinormal modes and a new instability of Einstein-Gauss-Bonnet black holes in the de Sitter world,” *Phys. Rev. D* **93** (2016) no.10, 104053, arXiv:1604.03604.
- [43] R. A. Konoplya and A. Zhidenko, “The portrait of eikonal instability in Lovelock theories,” *JCAP* **1705** (2017) no.05, 050, arXiv:1705.01656.
- [44] R. Bousso and S. W. Hawking, “Pair creation of black holes during inflation,” *Phys. Rev. D* **54** (1996) 6312-6322, arXiv:gr-qc/9606052.